Flexural Behavior of Self Compacting Concrete T-Beams Reinforced with AFRP

Sinan Abdulhkaleq Yaseen[1]

[1] Civil Engineering Department, Salahaddin University-Erbil, Iraq
Correspondence: Sinan Abdulhkaleq Yaseen, Salahaddin University, Erbil, Iraq
Email: sinan_abd@yahoo.com

Received: October 9, 2018 Accepted: November 20, 2018 Online Published: December 1, 2018

doi: 10.23918/eajse.v4i2p178

Abstract: In this paper, an experimental work is carried out to study behavior and performance of Self compacted reinforced concrete (SCC) T-section beams reinforced with Aramid fiber reinforced polymers (AFRP). Key variables taken into consideration were flexural reinforcement ratio, and different self-compacting concrete mixes having different strengths. Normal strength steel bars was witnessed for data comparison. 9 samples of T-sections were designed using (AFRP) to be weak in flexure. 3 samples of T-sections were used with normal steel bars as control samples for comparison. The effect of these fiber reinforcement contents on flexural behavior and crack pattern were observed during third-point loading tests. A data comparison was performed between experimental and analytical beam calculation using ACI 440 as an applied design source. The results show that the final deflection was more in AFRP compared with steel reinforced beams indicating to significant enhancement in strength and toughness. The ultimate capacity of AFRP beams increased more than steel reinforced beams by increasing self-compacting concrete strength. The reinforcement ratio improves the final resisting load as the ratio increases. The maximum observed crack-width in beams reinforced with AFRP bars is three to five times that of normal steel reinforced beams. The exactness of the data depends on both the compressive strength and reinforcement ratio for both AFRP and conventional steel bars. It is seen from data compared with experimental work the ACI 440 method was more conservative when using AFRP reinforcement and SCC.

Keywords: T-Beam, Aramid Fiber Reinforced Polymer, Flexural Behavior and Performance, Self-Compacting Concrete

1. Introduction

T-shaped beam is produced as a combination slab beam action in reinforced concrete system as they placed monolithically; these two parts acts together to resist flexural and shear stresses (Daia & Thomas, 2002; Guowei et al., 2011; Tiago et al., 2010; Erki & Rizkalla, 1993). Self-Consolidating Concrete (SCC) become popular in construction industry. Because of high flowability and moderate viscosity, no blocking may occur during flow; which has to de-air by itself during casting of SCC. It is used in specific structures instead of the conventional type concrete (Yasser, 2012; Raya & Bilal 2015). Here the most point of concern in concrete structures is the durability. Corrosion of steel reinforcement (main element in casting members) is related to durability problem. Corrosion attacked constructions are chemical industry facilities, coastal structures, bridges, and ports; they are examples of critical structures subject to reinforcement corrosion. Different types of reinforcements are used to fill the tension weakness side of concrete, such as fiber-reinforced polymers (FRP), glass fiber reinforced polymers (GFRP), and aramid fiber reinforced polymers (AFRP). The main

advantage of these materials than conventional reinforcement is corrosion resistance, it can be used in magnetic field area, and has high strength-to-weight ratio (Rolland et al., 2014; Efe & Head, 2014; Ola & Jonas, 1993). AFRP bars are made of composite fibers and possess numerous other distinct properties such as excellent fatigue behavior, high tensile strength, and non-conductivity, while their thermal expansion is close to that of concrete. These bars govern structural behavior of casted elements when subjected to flexural stresses. The elastic modulus, tensile strength, and bond properties are the main mechanical properties of AFRP (Rolland et al., 2014; Ola & Jonas 1993; ACI 440.1R, 2006). Up to date, very little work has investigated the flexural behavior and performance of T-beams reinforced with AFRP and casted by Self compacted concrete. Lee et al. (2011) investigated the externally strengthened T-beam behavior in shear and the performance of these beams. It was concluded that the strengthening length of the sheets, fiber direction combination, and anchorage have significant influence on the shear performance of strengthened deep beams. Tavares et al. (2008) studied the behavior of reinforced concrete beams reinforced with GFRP bars. They show that the capacity of the beams was lower than that of the steel-reinforced beam and it seen that similar flexural capacity can be achieved for the steel- and for the GFRP-reinforced concrete beams by controlling the stiffness. Buyukkaragoz et al. (2013) made a numerical study of concrete beams reinforced with AFRP bars to focus on the flexural behavior. The load on the beams found by finite elements FE was near to those from the effective moment of inertia expressions, the numerical ultimate moments also correlated well with the analytical values of concrete stress-strain models. Numerical analyses, which hardly predict the sudden reduction in the flexural rigidity of FRP-reinforced concrete beams due to the crushing of cover concrete, were shown to provide somewhat conservative deflection estimates.

2. Research Significance

In the present study, series of T-beams were tested to investigate the flexural behavior of T-section casted with SCC and reinforced with AFRP bars, to show their influence on load carrying capacity, toughness, and changing of properties while comparing with normal concrete with conventional steel bars. A total of 12 T-beams sections (9 reinforced by AFRP and 3 with steel bars) were designed to be deficient in flexure. The behaviors of the tested beams were studied during static third -point loading tests with crack patterns. The flexural behaviors were observed from the load-displacement curves. In addition, a comparative study was made between the present experimental results and theoretical results based on ACI440 (ACI440, 2006).

3. Experimental Program

The test program include fabrication of T-beams with three different compressive strengths of self-compacted concrete 60, 80, and 100 MPa, and using AFRP as main longitudinal reinforcement with different ratios (less than balance reinforcement, between balance and $1.4\rho_b$ ratio, and more than $1.4\rho_b$). Also three beams were casted using conventional steel bars with balanced reinforcement ratio, as a reference

3.1. Details of Flexural -Deficient T-Beams

A total of 12 reinforced SCC T-beams, 3 normal reinforced with steel bars and the other with AFRP bars was designed and casted. T-beams dimension were: web width 75mm, flange width 200mm, flange thickness 50mm, over all height 200mm, with beam length of 1100mm as shown in Fig.1. The notation (TA) was given for Aramid reinforced samples, while (TS) was given for normal reinforced

samples. The reinforcing details of all the group samples are given in Table.1.

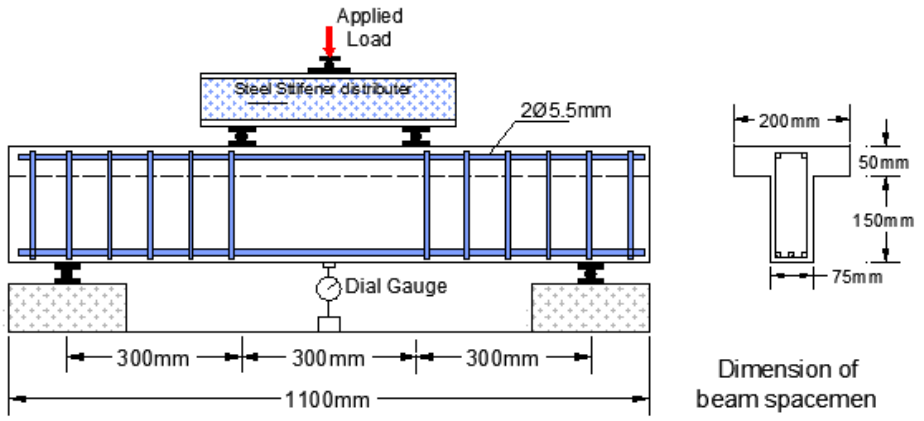

Figure 1: Tested beam geometry

Table 1: Tested beam details

G. No.	Sample	SCC strength $\acute{f}_c$ (MPa)	Rein.Ratio ρ	No. of main bars	Stirrups	Details
1	TS-11	60	0.83	2-Ø8mm	Ø5.5@ 75 mm	ρ_b
	TA-12		0.55	1-Ø5mm		$\rho < \rho_b$
	TA-13		1.09	2-Ø5mm		$\rho_b < \rho < 1.4\rho_b$
	TS-14		1.64	3-Ø5mm		$\rho > 1.4\rho_b$
2	TS-21	80	0.97	2-Ø10mm	Ø5.5@ 75 mm	ρ_b
	TA-22		0.82	2-Ø5mm		$\rho < \rho_b$
	TA-23		1.23	3-Ø5mm		$\rho_b < \rho < 1.4\rho_b$
	TA-24		1.64	4-Ø5mm		$\rho > 1.4\rho_b$
3	TS-31	100	0.78	2-Ø10mm	Ø5.5@ 75 mm	ρ_b
	TA-32		0.66	3-Ø5mm		$\rho < \rho_b$
	TA-33		1.31	4-Ø5mm		$\rho_b < \rho < 1.4\rho_b$
	TA-34		1.64	5-Ø5mm		$\rho > 1.4\rho_b$

3.2. Details of Self Compacted Concrete

Control specimens' properties of the SCC in fresh state and hardened state were studied through a series of casting and testing of concrete specimens Table (2). Properties of SCC in fresh state which includes: slump flow test which investigate the filling ability and flow time (T50), The V-funnel test which measures the flow time for SCC needs to pass a narrow opening that show the filling ability blocking and/or segregation do not take place, and L-box test which measures the reached height of fresh SCC in the formworks, were examined and listed in Table (3). In the hardened state, the compressive strength and modulus of elasticity tests were carried out.

Table 2: Self-compacted concrete mix proportion

Mix No.	Cement kg/m3	Gravel kg/m3	Sand kg/m3	Silica Fume kg/m3	Stone Powder kg/m3	%Super plasticizer By weight of cement	Free water kg/m3	SCC strength at 28 day f_c (MPa)
Mix 1	380	850	900	38	57	1.40	155	60
Mix 2	440	800	900	44	66	1.20	165	80
Mix 3	480	900	720	48	72	2.10	139	100

Table 3: Fresh self-compacted concrete test results

Mix No.	Slump Flow (mm)	T_{50} (sec)	V-Funnel (sec)	L-Box (H1/H2)
Mix 1	645	4.45	9.65	0.88
Mix 2	675	3.12	8.4	0.91
Mix 3	565	6.85	12.32	0.8

4. Results Evaluation

4.1 Outcome Results

The results of all specimens with their 1st cracking load, deflection, ultimate load (P_u), and there final deflections are summarized in Table 4.

Table 4: Tests results of SCC T-Beams

Sp.No.	G.No.	Samples	SCC strength f `c (MPa)	First Crack load kN	Deflection at first crack mm	Failure load kN	Deflection mm
1	G1	TS-11	60	21.07	1.4	52.67	5.99
2		TA-12		7	3.17	33.6	79.11
3		TA-13		8.64	5.9	60.45	87.26
4		TA-14		9.82	6.2	70.7	91.61
5	G2	TS-21	80	22.69	0.91	75.64	5.96
6		TA-22		4.76	2.9	65.03	80.55
7		TA-23		6.86	3.8	84.38	83.06
8		TA-24		10.16	5.27	94	89.15
9	G3	TS-31	100	23.47	0.91	78.25	5.03
10		TA-32		8.08	1.22	95.35	81.98
11		TA-33		9.13	3.2	107.57	85.19
12		TA-34		9.37	3.53	119.93	91.2

4.2 Crack Pattern and Modes of Failure

The flexural crack of the T-beam specimens starts at the bottom close to midspan of beam when the applied load reached the values shown in Table 4. The first crack load increased slightly when the concrete strength changed from 60 to100MPa for the same reinforcement ratio. Steel reinforced specimens had very lesser deflection at first crack at very higher loads compared with aramid

reinforced beams. Number of cracks increases by load increasing and extend upward, indicating the neutral axis movement upward as shown in Fig. 2. Further loading on specimens, cracks propagated typically as for ordinary flexural beams. The cracks at the failure stage in the AFRP reinforced beam were mainly vertical cracks under the applied load. These cracks had similar shape but larger width than the cracks in the steel reinforced beam. The final crack spacing approximately was 2.3, 3.4, 5.8 mm for the three ratios respectively. The maximum observed crack-width in beams reinforced with AFRP bars is three to five times that of normal steel reinforced beams. In contrast, the cracks in the steel-reinforced beam were mainly one vertical and two inclined cracks; all of them started from bottom and moved up to where the load line was imposed. Observation of the cracks shows that the crack propagation was much progressive on the AFRP beams than steel reinforced beam. The number of cracks was much larger in the AFRP specimens compared to the normal T-beams. All beams failed under compression failure at regions close to the loading points. On the normal beam, the failure was initiated by the yielding of the steel reinforcement and followed by the compression failure of the concrete. The final deflections of AFRP beam ranged between 80-90mm more than the steel reinforced beams which was 6 mm.

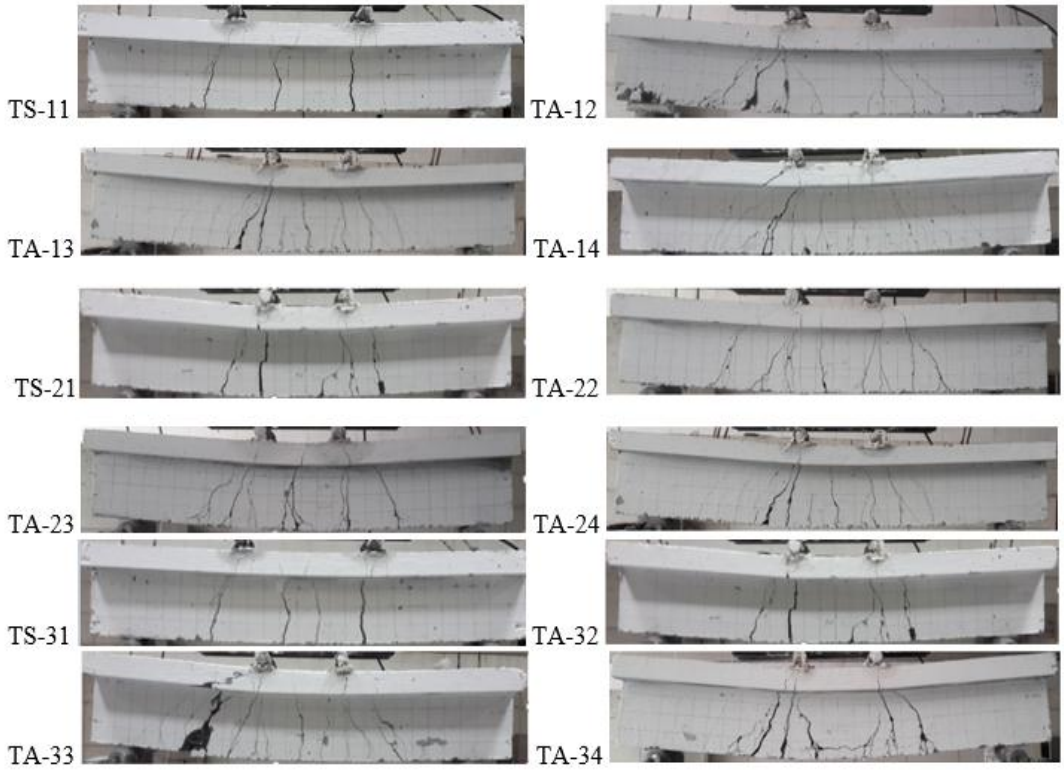

Figure 2: Crack pattern of T-beams

4.3 Compressive Strength Effects on Ultimate Capacity

A different group of T-beams with same reinforcement ratios are compared for each of the compressive strength of SCC taken in this paper. The increase of ultimate capacity seen to be small in low AFRP ratios and increased when the strength changed from 60MPa, to 80MPa, and then to 100MPa for reinforcement ratios listed in Table 1, respectively as shown in Fig. 3. The smooth increase of load carrying capacity is observed for the three samples of each strength indicated. The

AFRP and steel reinforced beams that have the same reinforcement ratio were compared, the steel reinforced beams load carrying capacity differs by 56.7%, 15.33%, and -17.93% than aramid reinforced beams respectively for concrete strength's groups. The steel reinforced beams show an increase of 43.6% in load carrying capacity when the concrete strength changed from 60 to 80 MPa and increase of 3.45% when the strength changed from 80 to 100 MPa.

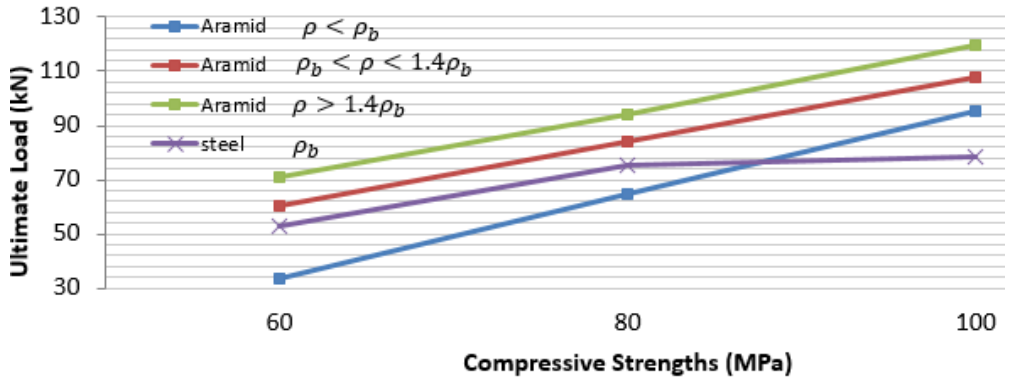

Figure 3: Ultimate load capacity vs SCC strength

4.4 AFRP Reinforcement Ratio Effect

Three beams were reinforced with ratios ($\rho < \rho_b$, $\rho_b < \rho < 1.4\rho_b$ and $\rho > 1.4\,\rho_b$ for each SCC concrete type. Three beams were reinforced with normal strength steel bar having balanced ratio of reinforcement for comparison purposes were tested under static loading conditions. The reinforcement ratio improves the final resisting load as the ratio increase. The increase was 79.9%, 29.7%, and 12.8% for each compressive strength group when the ratio changed from $\rho < \rho_b$ to $\rho_b < \rho < 1.4\rho_b$, and the increase were 16.9%, 11.4%, and 11.4% for each compressive strength when the ratio changed from $\rho_b < \rho < 1.4\rho_b$ to $\rho > 1.4\,\rho_b$ as shown in Fig. 4.

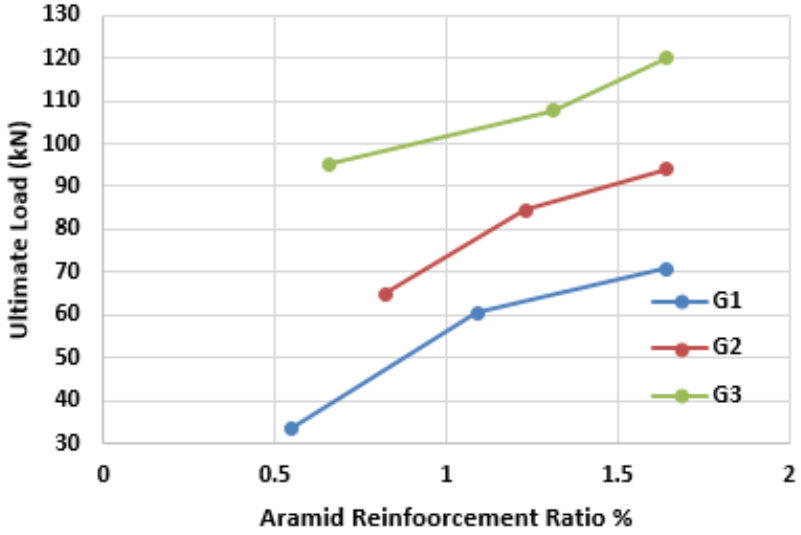

Figure 4: Ultimate load capacity vs AFRP ratio

4.5 Load Displacement Relations

The relationships between applied load stages and their deflection response at the mid span are shown in fig. 5, 6, 7 for AFRP reinforced beams, and Fig.8 for steel reinforced beam. An extensive deformation was noted at failure as shown in Fig. 2 and Fig. 5, 6, 7 in aramid beams and the effect of increasing the AFRP ratio had slight influence on reducing the deflections in the beams; these are due the low elastic modulus of AFRP. The increase of the reinforcement ratio had an effect of increasing the ultimate load capacity of the beams. A very small deflection was seen in normal strength steel reinforced beams with a moderate final load carrying capacity. The deformed Steel bars carry a load better than AFRP because it is stiffer. From a large load carrying intensities shown, it is concluded that the AFRP bars develop high tensile stress like steel bars higher at high strain levels. An increase in load carrying capacity was seen in comparison of similar AFRP ratio groups by changing the concrete strength. For $\rho < \rho_b$ group an increase in load were 93.5% and 46.6% when the strengths changed from 60-80 MPa and 80-100 MPa respectively, for $\rho_b < \rho < 1.4\rho_b$ group an increase in load was 39.58% and 27.4% when the strengths changed from 60-80 MPa and 80-100 MPa respectively, and for $\rho > 1.4\,\rho_b$ group an increase in load was 32.95% and 27.58% when the strengths changed from 60-80 MPa and 80-100 MPa respectively. The displacements in steel reinforced beams were too smaller compared with AFRP beams. The displacements reduced with increasing the concrete strength, but the load carrying capacity increased with increasing the SCC strength as seen in Fig. 8.

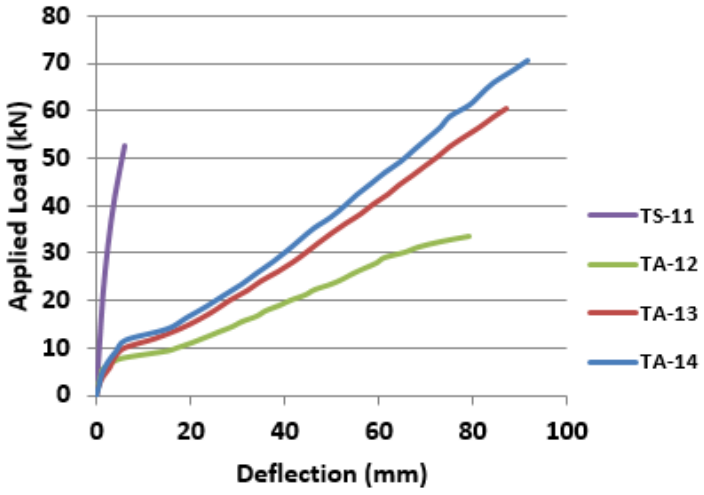

Figure 5: Force-Displacement response for G1- $\acute{f}_c$ = 60MPa Aramid and steel reinforced T-beams

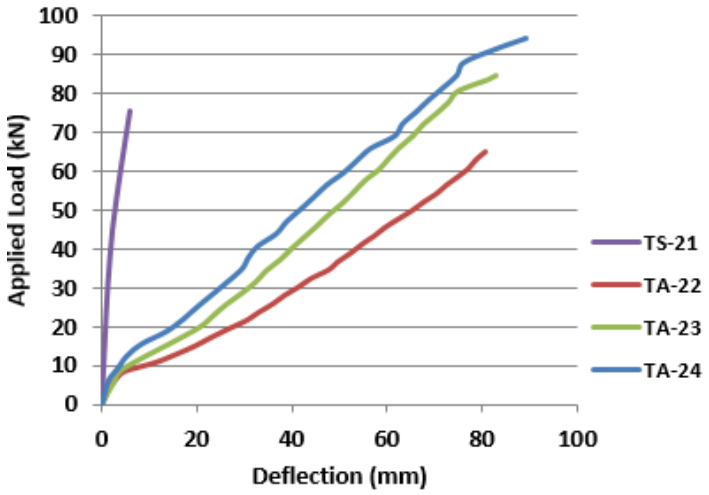

Figure 6: Force-Displacement response for G2- $\acute{f}_c$ = 80MPa Aramid and steel reinforced T-beams

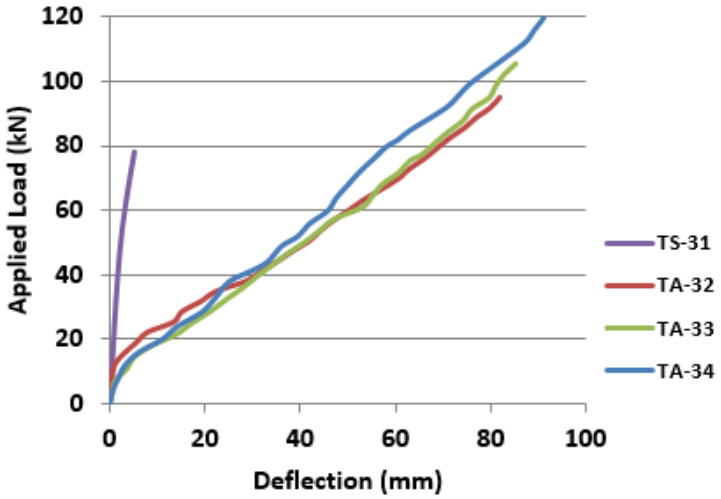

Figure 7: Force-Displacement response for G3- $\acute{f}_c$ = 100MPa Aramid and steel reinforced T-beams

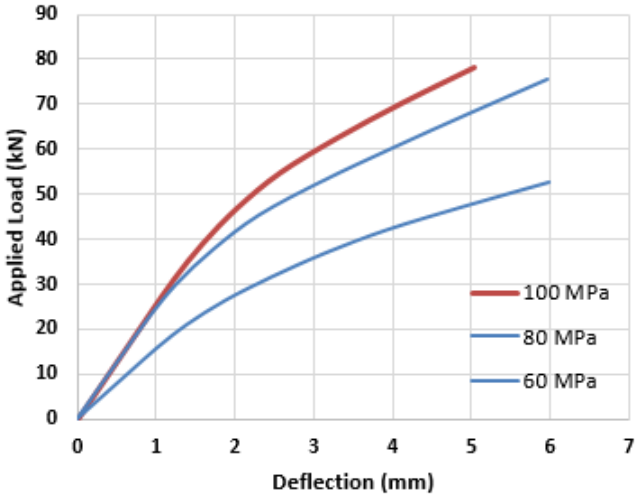

Figure 8: Force-Displacement response for steel reinforced T-beams

5. Theoretical Stress Block Evaluation

When the neutral axis depth lay within the flange of T-beam ($a \leq$ hf), it means the beam acts as a rectangular section with a width of the concrete compression block is equal to the b_f (flange width), Fig. 9. The neutral axis depth c (and consequently the equivalent stress block evaluated) is found from the axial force and moment equilibrium equations. The value of (a) for the concentric loading cases of T-beam increases as the concrete strength increases (related to strain value) or vice versa. It can be easily observed from Fig.10 that the SCC compressive strength affects the values of (a) for the same reinforcement ratio groups (Aramid & Steel). An increase in block depth was observed by increasing the strength of concrete for AFRP $\rho < \rho_b$ and steel $\rho = \rho_b$, while it Noted that the depths for AFRP $\rho_b < \rho < 1.4\rho_b$ and $\rho > 1.4\rho_b$ were too large and equal for the same group of reinforcement ratio. The effect of reinforcement ratio on the values of (a) for the same groups of SCC compressive strength is shown in fig.11. It is recorded that there is a significant increase in the depth of compressive stress by increasing the reinforcement ratio for all AFRP samples.

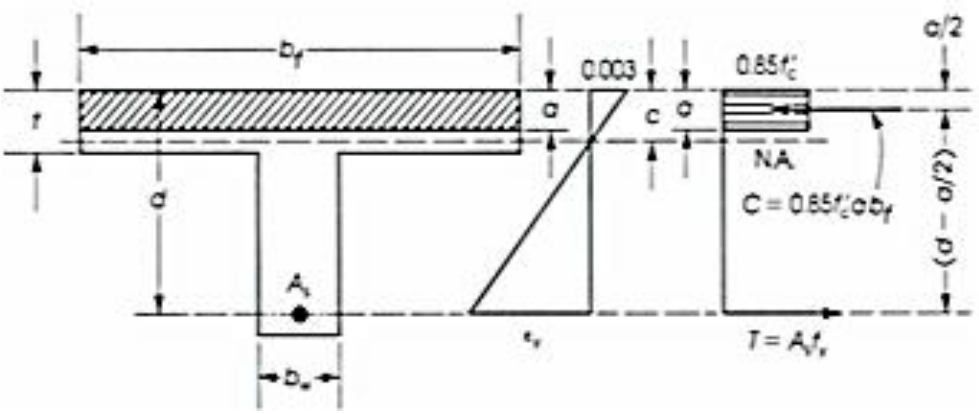

Figure 9: Flanged T-beam ($a \leq h_f$)

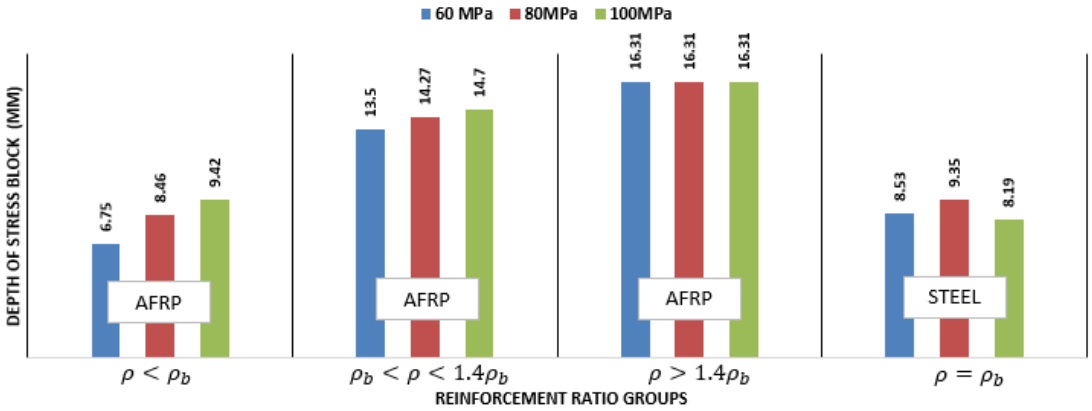

Figure 10: Effect of SCC compressive Strength on Equivalent stress block

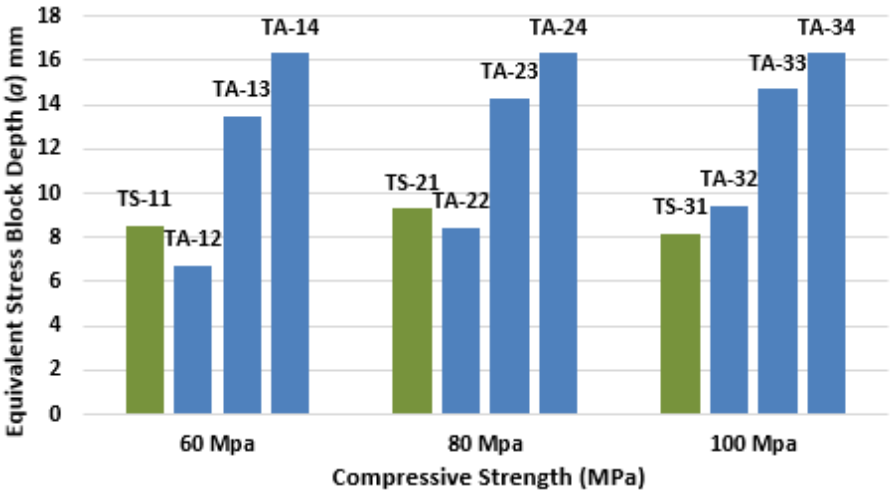

Figure 11: Effect of reinforcement ratio of (Aramid & Steel) on depth of Equivalent stress block

6. Analytical Methods for Comparison Using ACI440-06

The difference in properties of used bars AFRP and normal steel, leads to obtain different strengths and strains which affects the determination of actual and balanced reinforcement ratio, and consequently, affected on equivalent stress block depth. The depth of stress block and the ultimate moment capacity for the under reinforced (for all types of reinforcement) are found by using conventional ACI 440 equations (Eq 1 & 2).

$$\epsilon_s \geq \epsilon_y \;; \qquad c = \frac{a}{\beta_1} \quad ; \quad \epsilon_s = \left(\frac{d-c}{c}\right)\epsilon_{cu} \geq \epsilon_y \qquad ; \qquad a = \frac{A_s f_s}{0.85 f'_c b} \qquad \textit{Eq.1}$$

$$M = A_s.f_s.\left(d - {}^{a}/_{2}\right) = \alpha_1.f'_c.a.b.\left(d - {}^{a}/_{2}\right) \qquad \textit{Eq.2}$$

The experimental versus the theoretical data for comparison are presented in Fig. 10,11,12,13, & 14. Ultimate load capacity versus SCC strength and reinforcement ratio are plotted for AFRP and normal steel reinforced T-beams. It is observed that as the SSC strength increases, the load carrying capacity increases. The increase in the reinforcement ratio ($\rho < \rho_b$, $\rho_b < \rho < 1.4\rho_b$ and $\rho > 1.4\,\rho_b$) leads to increase the load capacity as well. From the plotted relation it is seen that there is good agreement between the experimental and theoretical results with increasing compression strength. Similar relation is seen between the experimental and theoretical data for conventional steel bars. It is seen that the ACI440 method was more conservative.

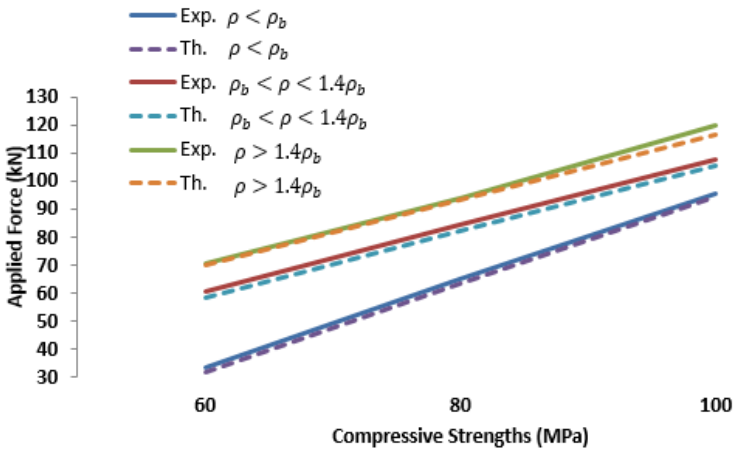

Figure 10: Analytical and experimental beam capacity vs SCC strength

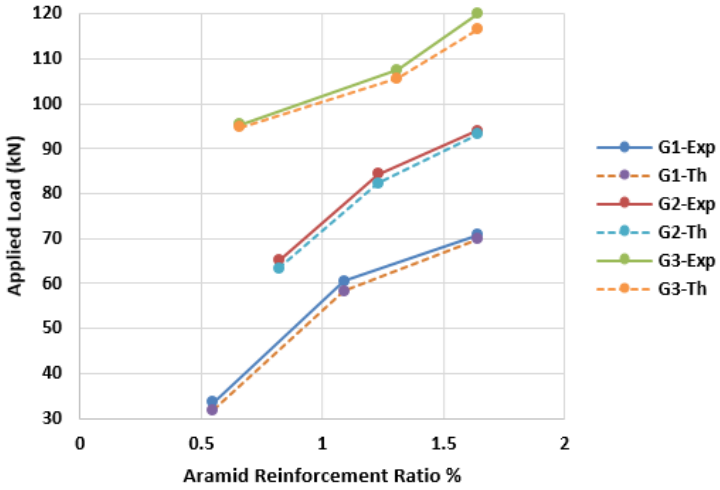

Figure 11: Analytical and experimental beam capacity vs Reinforcement Ratio

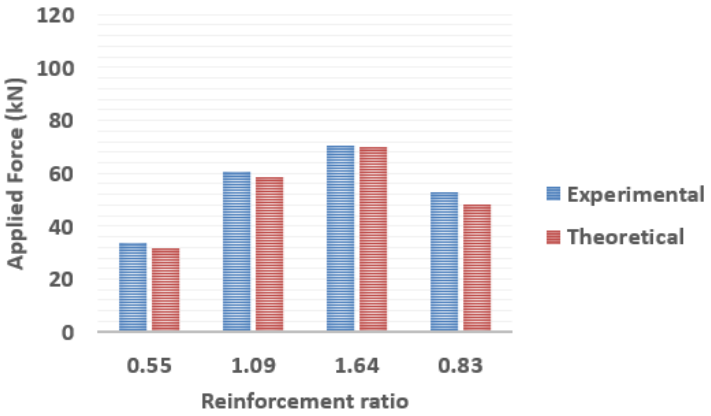

Figure 12: Analytical and experimental beam capacity vs Reinforcement Ratio for G1-$\acute{f}_c$=60MPa

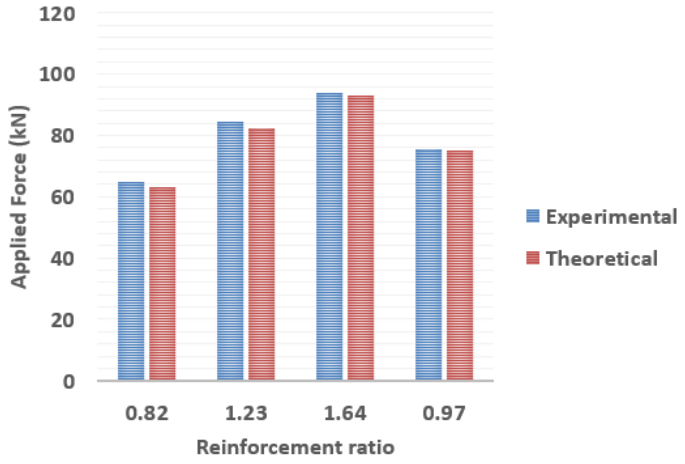

Figure 13: Analytical and experimental beam capacity vs Reinforcement Ratio for G2-$\acute{f}_c$=80MPa

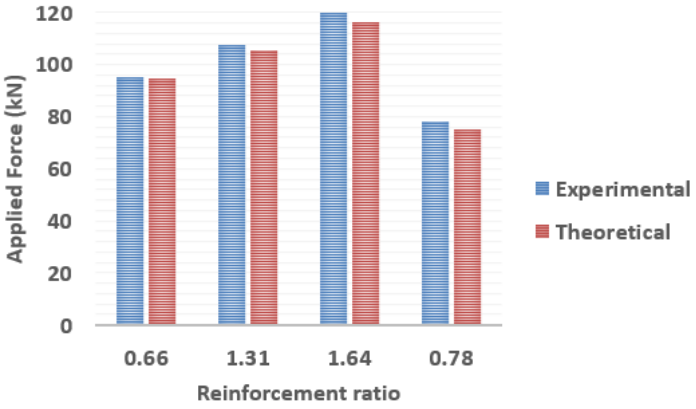

Figure 14: Analytical and experimental beam capacity vs Reinforcement Ratio for G3-$\acute{f}_c$=100MPa

7. Conclusion

1-The final deflection increases with the increase of the reinforcement ratio for the three group ($\rho < \rho_b$, $\rho_b < \rho < 1.4\rho_b$ and $\rho > 1.4\,\rho_b$), while the deflection was limited in the deformed normal steel bar reinforced beams, which reflects to toughness enhancement compared with steel bars.

2- An increase in load carrying capacity were seen in comparison of similar AFRP ratio groups by changing the concrete strength, for $\rho < \rho_b$ group an increase in load were 93.5% and 46.6% when the strengths changed from 60-80 MPa and 80-100 MPa respectively, for $\rho_b < \rho < 1.4\rho_b$ group an increase in load were 39.58% and 27.4% when the strengths changed from 60-80 MPa and 80-100 MPa respectively, and for $\rho > 1.4\,\rho_b$ group an increase in load were 32.95% and 27.58% when the strengths changed from 60-80 MPa and 80-100 MPa respectively.

3- The steel reinforced beams load carrying capacity differs by 56.7%, 15.33%, and -17.93% than aramid reinforced beams for all concrete strength's groups for balanced reinforcement ratio.

4-The steel reinforced beams show an increase of 43.6% in load carrying capacity when the concrete

strength changed from 60 to 80 MPa and increase of 3.45% when the strength changed from 80 to 100 MPa.

5- The reinforcement ratio improves the final resisting load as the ratio increases. The increase was 79.9%, 29.7%, and 12.8% for each compressive strength when the ratio changed from $\rho < \rho_b$ to $\rho_b < \rho < 1.4\rho_b$. and the increase were 16.9%, 11.4%, and 11.4% for each compressive strength when the ratio changed from $\rho_b < \rho < 1.4\rho_b$ to $\rho > 1.4\,\rho_b$.

6-The final crack spacing approximately were 2.3, 3.4, 5.8 mm for the three ratios respectively. The maximum observed crack-width in beams reinforced with AFRP bars is three to five times that of normal steel reinforced beams.

7- In theoretical calculation, an increase in block depth was obtained when increasing the strength of concrete for AFRP $\rho < \rho_b$ and steel $\rho = \rho_b$, while the depths for AFRP $\rho_b < \rho < 1.4\rho_b$ and $\rho > 1.4\rho_b$ were too large and equal for the same group of reinforcement ratio.

8- It is from data comparison with experimental work that the ACI440 method was more conservative when applied on SCC AFRP reinforced beams.

References

ACI 440.1R-06. (2006). ACI Committee 440 Guide for the Design and Construction of Concrete Reinforced with FRP Bars, American Concrete Institute, Farmington Hills, Michigan.

Buyukkaragoz, A., Kalkan, I., & Lee, J. H. (2013). A Numerical Study of the Flexural Behavior of Concrete Beams Reinforced with AFRP Bars. *Strength of Materials Journal*, 45(6), 716–729.

Daia, Z., & Thomas, V. (2002). Checking the Limit State of Existing T-Beam Girder Bridges. 6th International Conference on Short & Medium Span Bridges SMSB-VI, Vancouver BC, Canada, 1, 691-698.

Efe, S., & Head, M. (2014). Structural behavior and response analysis of aramid fiber reinforced polymer reinforced bridge columns under combined loading. Tenth U.S. National Conference on Earthquake Engineering Frontiers of Earthquake Engineering. Anchorage, Alaska.

Erki, M. A., & Rizkalla, S. H. (1993). FRP reinforcement for concrete structures. A sample of international production.

Guowei, N., Bo, L., Xiao L., & Wenshang, Y. (2011). Experimental Study on concrete T-Beams strengthened with Carbon Fiber reinforced Polymer (CFRP) Sheets on Three Sides. *Systems Engineering Procedia*, 1, 69–73.

Lee, H. K., Cheong, S. H., Ha, S. K., & Lee, C. G. (2011). Behavior and performance of RC T-section deep beams externally strengthened in shear with CFRP sheets. *Journal of Composite Structures*, 93, 911–922.

Ola G., & Jonas H. (1993). Aramid Fiber Rods as Reinforcement in Concrete. Lund Institute of Technology, Department of Structural Engineering, Report TVBK-5067, Sweden.

Raya, H. H., & Bilal, S. H. (2015). Performance of high strength self-compacting concrete beams under different modes of failure. *International Journal of Concrete Structures and Materials*, 9(1), 69–88.

Rolland, A., Chataigner, S., Benzarti, K., Quiertant, M., Argoul, P., & Paul, J-M. (2014). Mechanical behaviour of aramid fiber reinforced polymer (AFRP) rebar/concrete interfaces. Transport Research Arena, Paris.

Tavares, D. H., Giongo, J. S., & Paultre, P. (2008). Behavior of reinforced concrete beams reinforced with GFRP bars. *IBRACON Structures and Materials Journal*, 1(3), 285 – 295.

Tiago, C., Carlos, C., & Hugo, B. (2010). Raquel Fernandes Paula. Flexural Behavior of RC T-

Beams Strengthened with Different FRP Materials. The Third International fib Congress and Exhibition "Think Globally, Build Locally".

Yasser, S. (2012). Structural performance of Self-Consolidating Concrete used in reinforced concrete beams. *KSCE Journal of Civil Engineering*, 16(4), 618–626.